JOURNAL OF MATERIALS SCIENCE **34** (1999) 1407–1415

Miscibility and morphology of poly p-phenylene sulphide–liquid crystal polymer blends

M. GOMES, M. SCUCCUGLIA, R. E. S. BRETAS*
Department of Materials Engineering-UFSCar, São Carlos, SP, Brasil
E-mail: bretas@power.ufscar.br

Blends of poly p-phenylene sulphide (PPS) and a liquid crystalline polymer (LCP) were made by two methods: (i) mixing and capillary extrusion (samples A), and (ii) injection moulding (samples B). To study miscibility in the melt and solid states and the resulting morphology, techniques like polarized light optical microscopy, capillary rheometry, dynamic mechanical thermal analysis and scanning electron microscopy with X-ray microanalysis were used. It was observed that the miscibility of the amorphous fractions of both polymers increased with increasing intensity (rates and stresses) of deformational flow (shear and elongational). Samples A had a morphology composed of fibrils of both polymers, but a matrix made of only one polymer i.e. PPS. Samples B had a mainly fibrillar morphology, with no observable matrix, made of both polymers. Formation of pure LCP fibrils was not observed neither in the extruded blends nor in the injection moulded samples. The addition of LCP to PPS improved its mechanical properties. At a molecular level, these blends can be considered to be "molecular composites". © *1999 Kluwer Academic Publishers*

1. Introduction

Poly p-phenylene sulphide (PPS) belongs to the so-called engineering thermoplastics class. Due to its chemical structure, made of phenyl groups linked by a sulfur atom, it has excellent chemical and thermal properties. When carbon or glass fibres are added to this polymer, the result is a composite of outstanding mechanical properties. Blending with a liquid crystalline polymer (LCP) also produces a high performance composite [1, 2].

However, in this last case, like in any other composite, in order to obtain optimum mechanical properties, the fibre aspect ratio, L/D, of the LCP must be high and the fibre–matrix interface should be strong, i.e. the interface must be capable of transfering load (tension) from the matrix to the fibre [3], without itself breaking.

The obtention of LCP fibres or fibrils, in a blend with PPS or any other thermoplastic matrix is not always possible; it depends on certain factors [4–6] e.g.:

1. The viscosity ratio, $\lambda = (\eta_d/\eta_m)$, where η_d is the viscosity of the dispersed phase and η_m the viscosity of the matrix phase.
2. The elasticity ratio, $(\psi_1)_d/(\psi_1)_m$, where ψ_1 is the first normal stress coefficient of the dispersed, d, and matrix, m, phases, respectively.
3. The intensity and type of deformational field.
4. The concentration and miscibility of the LCP.
5. Interfacial tension, ν.

In other words, the production of a fibrillar phase will depend on the ratio between the shear and the cohesive forces, or the critical Weber number, $We = (\eta_m \dot{\gamma} d/\nu)$, where $\dot{\gamma}$ is the shear rate and d the initial diameter of the dispersed phase.

In conventional blends, when $\nu \to 0$ and $\lambda < 1$, it is usually observed that small fibres or droplets will be formed only at high shear rates; when $\lambda > 1$, fibrils of higher diameter will be produced only in extensional flow [4, 7]. In the case of thermoplastics–LCP blends, it is observed that shear deformation is not as effective on promoting LCP fibrillation as is steady elongational deformation. The concentration of the LCP is also important. It seems that below a critical concentration, C^*, no fibrils will be formed [8, 9].

The miscibility seems to play a minor role; it is believed that miscibility will make formation of the fibrils difficult, because dispersion of LCP macromolecules into the thermoplastic matrix will diminish the probability of LCP domain formation and, therefore, of the formation of LCP fibrils. However, some studies [5, 8] have shown that even in miscible blends, small fibrils (0.4 μm in diameter), made of both components (polyetheretherketone, PEEK, and HX4000, a LCP from DuPont) are formed above a certain C^*, even when $\lambda > 1$. When the blends are immiscible, like blends of PPS and HX4000, the final morphology depends primarily on C^*; thus, in these blends the formation of droplets (0.2–1.0 μm) and fibrils (0.6–1.0 μm) is observed below 40 wt % LCP concentration and at $\lambda < 1$. However, only fibrils (0.1 μm) are formed above this concentration, when $\lambda > 1$ [8, 9]. Because these blends were made by injection molding, which has deformational fields composed of shear and elongation, it is

* Author to whom correspondence should be addressed.

difficult to investigate the influence of each factor separately. Therefore, due to the fact that there are many variables that, jointly, determine the production of fibrils in a blend with LCP, we have undertaken this study. We will analyse the influence of the viscosity ratio, deformational field, concentration and miscibility of the LCP on the production of fibrils. The influence of elasticity and interfacial tension will be the subject of future work.

2. Experimental procedure

2.1. Materials

The PPS used was Fortron 0205B4 and the LCP was Vectra A950, (Hoechst). Vectra is a random copolyester made of 75 mol % 4-hydroxybenzoic acid and 25 mol % 2-hydroxy-6-naphtoic acid.

2.2. Blending

Two kinds of blends were prepared, all based on volume fractions; the PPS–LCP ratios were: 70 : 30, 50 : 50 and 30 : 70. Before blending, the component polymers were dried at 100 °C for 2 h.

Samples A were first mixed in a Haake Rheometer (System 90) using a closed batch mixer with a sigma rotor (Rheomix type 600), at 290 °C and 45 r.p.m. for 7 and 15 min. After mixing, the blends were pelletized using a blade mill; later, they were extruded in a capillary rheometer (Instron, model 3211) at a temperature, $T = 290\,^{\circ}\mathrm{C}$, using a capillary die of length, $L = 2.542\,\mathrm{cm}$ and diameter, $D = 0.1273\,\mathrm{cm}$ and $\theta = 90^{\circ}$. Capillary extrusion was done in order to assure that mainly deformational shear was acting on the blends.

Samples B were injection moulded in a Pic-Boy injection moulding machine. The average barrel temperature was 290 °C and the mould temperature was 25 °C. The injection pressures varied from 2.9×10^5 Pa (high LCP concentration) up to 6.9×10^5 Pa (low LCP concentration). The average injection time was 4–6 s. After injection moulding, samples B were annealed at 140 °C for 3.5 h, using a hot press.

2.3. Thermal transitions

The melting and cold crystallization temperatures of the homopolymers as-received were analysed using a differential scanning calorimeter (DSC-7, Perkin Elmer). The samples were first heated at $20\,^{\circ}\mathrm{C\,min^{-1}}$ up to 340 °C, held at this temperature for 1 min and later cooled to room temperature, also at a rate of $-20\,^{\circ}\mathrm{C\,min^{-1}}$. The secondary transitions of samples B were measured in a dynamic mechanical analyser (DMTA, Polymers Lab), on bending (double cantilever), at 1 Hz, strain of 64 μm and at a heating rate of $5\,^{\circ}\mathrm{C\,min^{-1}}$.

2.4. Mechanical properties

The tensile properties of samples B were measured using an Instron tensile machine, model 1127, at a crosshead speed of $2\,\mathrm{mm\,min^{-1}}$, following the procedures described in ASTM-D632. The notched impact properties of samples B were also measured using a Custom Scientific Izod impact equipment, following ASTM D256-1 standard procedure. Both tests were carried out at room temperature.

2.5. Microscopy

To observe miscibility in the melt state, a polarized light optical microscope (PLOM, Leica, model DMRXP) coupled with a hot stage (Linkam, THMS 600) were used. For better observation, the samples were initially ultramicrotomed using a Reichert Ultracut S/FCS ultramicrotome (Leica). Each sample was first melted at 350 °C, held at this temperature for 5 min and sheared with a glass slide; after melting they were cooled to room temperature at a rate of $-5\,^{\circ}\mathrm{C\,min^{-1}}$.

The morphology and composition of the blends in the solid state were analysed using a scanning electron microscope (SEM, Carl Zeiss, DSM 940 A), coupled with an X-ray microanalyser. The surfaces were prepared by breaking the samples in a liquid N_2 atmosphere and coating these surfaces with Au; the surfaces were perpendicular to the flow direction.

3. Results and discussion

3.1. Melt state

Fig. 1 shows a PLOM micrograph of a 50 : 50 PPS–LCP blend, at 350 °C, after being sheared. Two distinct phases are observed; the birefringent ones with a schlieren texture, belong to the LCP-rich phase and the transparent ones correspond to the PPS-rich phase. Evidently, the applied shear deformation is not as intense as the deformation found in extrusion and injection moulding. Therefore, this phase separation can be the result of the application of a small deformation. However, due to the low resolution of this microscopy technique, we cannot draw any conclusion about miscibility.

After cooling at $-5\,^{\circ}\mathrm{C\,min^{-1}}$, PPS begins to crystallize at around 210 °C. Fig. 2 shows this crystallization. Again, a two-phase region is observed: one composed of PPS-rich spherulites and the other of LCP-rich domains.

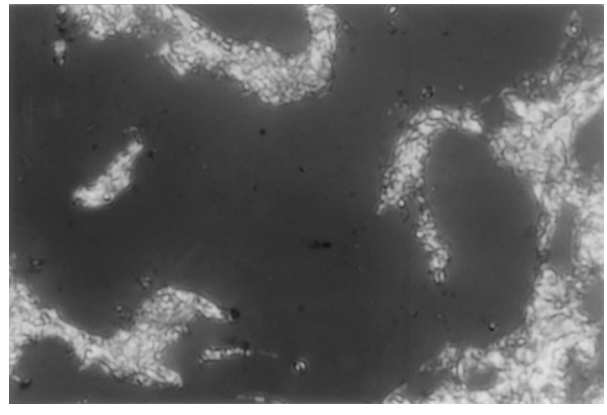

Figure 1 Polarized light optical micrograph of a 50 : 50 PPS–LCP blend, at 350 °C, after being sheared (magnification: ×400).

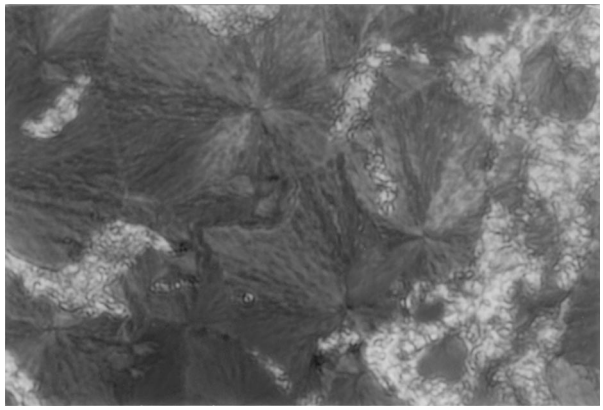

Figure 2 Polarized light optical micrograph of a 50 : 50 PPS–LCP blend, after crystallization at 210 °C (magnification: ×400).

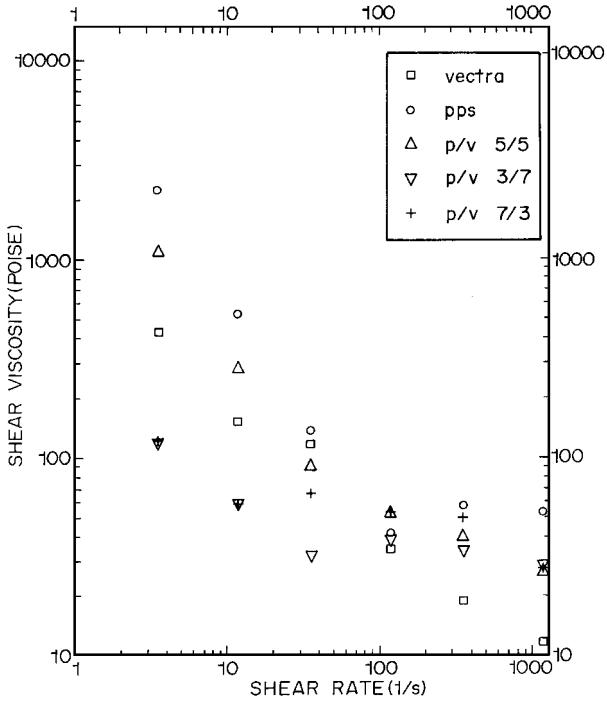

Figure 3 Steady shear viscosity of the pure polymers and their blends, at 290 °C.

The steady shear viscosity of samples A (7 min) are shown in Fig. 3, at 290 °C: the viscosities of samples A (15 min) are similar. Between the measured shear rate range of 1–1200 s^{-1}, PPS has a higher viscosity than LCP. Therefore, at low concentrations of LCP, where this polymer can be considered to be the dispersed phase, $\lambda < 1$, LCP fibrils will form if the shear rates are extremely high; at high concentrations of LCP, where this polymer can be considered to be the matrix phase, $\lambda > 1$, LCP fibrils will form only in extensional flow. The 70 : 30 and 30 : 70 PPS–LCP blends have lower viscosities than the pure components at low shear rates (1–10 s^{-1}); however, at moderate shear rates (100–1200 s^{-1}) they have intermediate values of viscosities. The 50 : 50 blend is observed to have an intermediate viscosity between both components at all shear rates. Therefore, LCP decreased the shear viscosity of PPS, independent of LCP concentration; this result allows us to conclude that miscibility between both components has occurred, due to the application of moderate and high shear deformation.

3.2. Solid state

3.2.1. Thermal transitions

Fig. 4 shows the heating and cooling DSC scans of both polymers, and Table I presents a summary of these transitions.

It can be observed that PPS melts at a higher temperature than LCP. Therefore, at and above 290 °C, LCP is a nematic liquid, while PPS is an isotropic melt. For this reason, LCP domains plasticized PPS entangled macromolecules, in the melt state. It is also observed that PPS will crystallize before LCP; this fact will affect both morphologies and crystallization kinetics of the polymers, as observed in a recent study [10] made on immiscible blends of PPS with HX4000. In this last mentioned study, it was found that due to the fact that PPS crystallized after HX4000, the presence of already crystalline HX4000 domains accelerated the PPS crystallization process (the HX4000 domains acted as nucleation agents for the PPS macromolecules). This

TABLE I Main thermal transitions[a] as measured by DSC at 20 °C min^{-1}

Transition	Vectra	Transition	PPS
Temperature, °C			
T_{CN}	283.20	T_m	299.66
T_{CC}	232.85	T_{CC}	243.45
Enthalpy, J g^{-1}			
ΔH_{CN}	1.062	ΔH_m	63.56
ΔH_{CC}	3.078	ΔH_{CC}	55.87

[a]CN, crystalline–nematic transition; CC, cold crystallization; m, melting.

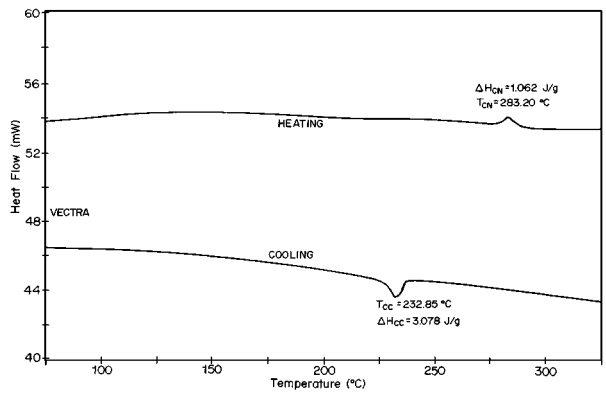

(a)

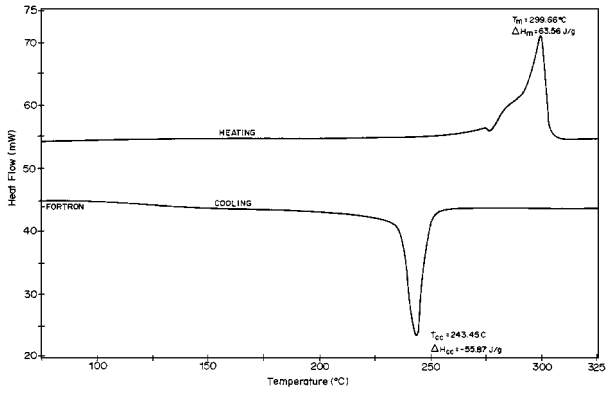

(b)

Figure 4 Differential scanning calorimetry of the pure polymers: (a) pure Vectra, and (b) pure PPS.

influence was also found in a study of miscible PEEK–HX4000 blends [11]. In this study, it was observed that PEEK crystallized before HX4000; thus, in this case, it was PEEK that acted as the nucleating agent for the HX4000 rigid macromolecules. We can conclude, therefore, that probably, in the present case, PPS will affect LCP crystallization kinetics and, consequently, its final morphology. However, this observation will need further DSC measurements.

Fig. 5 shows a typical DMTA run of the blends (samples B) and pure components, and Table II presents a summary of these transitions. DMTA of samples A was not done, because of the fragility of the extrudates. The standard deviation of each average is given in parenthesis.

These values were taken at the temperatures where the loss modulus, E'', has a maximum. The β-transition of this LCP can be attributed to relaxation of the naphthoic unit; this has also been found in other LCPs [12]. It can be observed that this transition changes slightly with blending with PPS. At high concentrations of PPS, it has values slightly above the β-transition of

TABLE II Secondary transitions[a] as measured by DMTA at 5 °C min^{-1} (samples B) of PPS–Vectra blends

	T_β (°C)	T_α (°C)	$T_{\alpha'}$ (°C)
100 : 0	—	120.44 (4.35)	—
70 : 30	35.10 (1.82)	116.66 (4.47)	221.93 (1.56)
50 : 50	34.60 (3.42)	117.54 (4.34)	215.83 (4.87)
30 : 70	30.95 (2.30)	109.52 (1.72)	207.23 (3.65)
0 : 100	32.40 (2.34)	105.92 (1.75)	220.46 (4.10)

[a] T_β, temperature at the β-transition; T_α, temperature at the α-transition; $T_{\alpha'}$, temperature at the α'-transition.

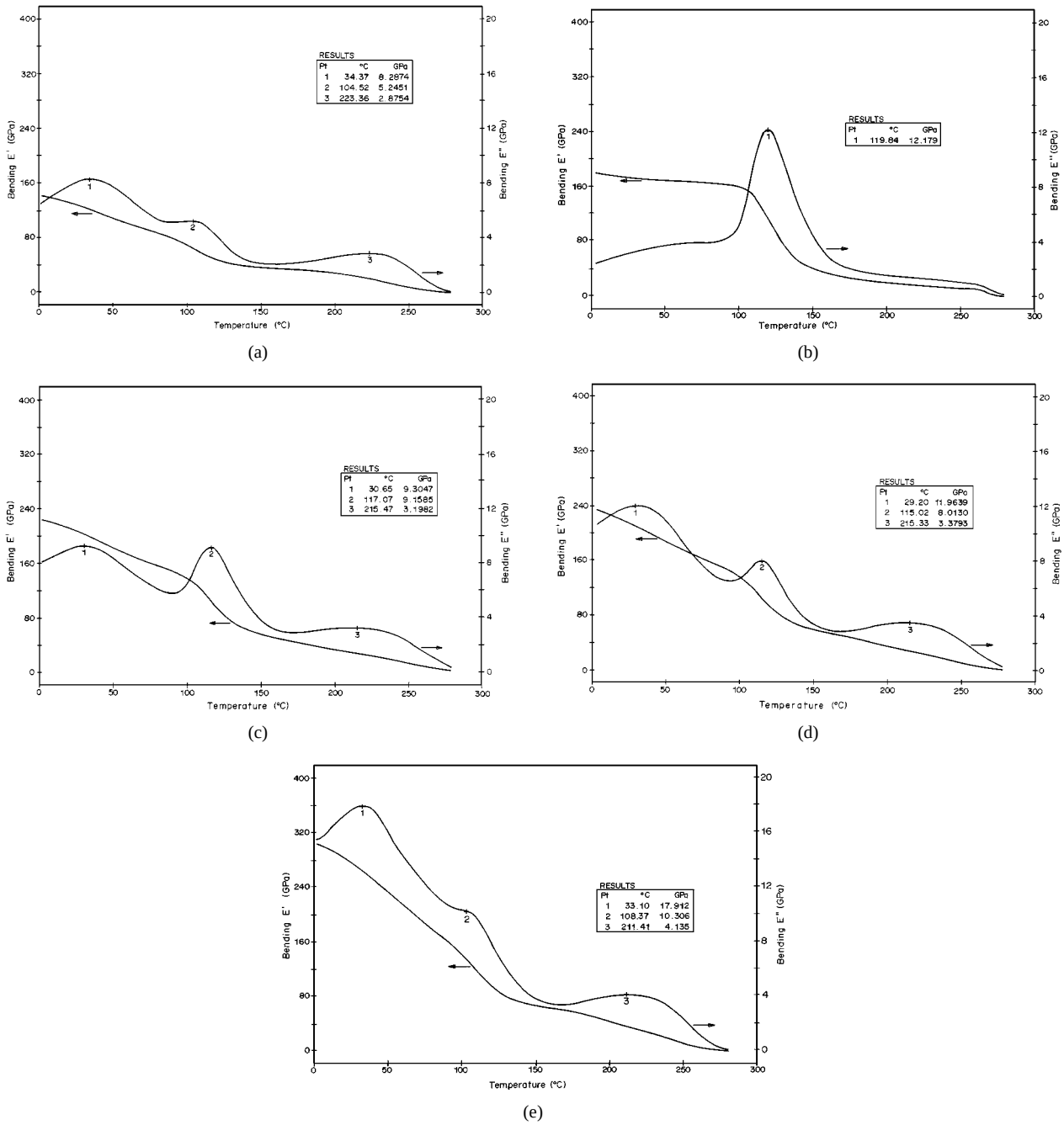

Figure 5 Typical DMTA scans of the pure polymers and their blends: (a) pure Vectra, (b) pure PPS, (c) 70 : 30 PPS–LCP blend, (d) 50 : 50 PPS–LCP blend, and (e) 30 : 70 PPS–LCP blend.

pure LCP, indicating that interactions of short range between the LCP naphthoic units and the PPS phenyl groups has occurred; this specific interaction can be due to the formation of n$-\pi$ (C=O and phenyl) or $\pi-\pi$ (phenyl–phenyl) complexes [13]. The interactions can occur if the LCP is miscible and disperses into the PPS matrix, where each rigid LCP macromolecule will be surrounded by many PPS macromolecules.

The LCP α'-transition is related to interdomain relaxation (similar to interspherulite relaxation). This α'-transition has the same behaviour with blending as the β-transition.

The α-transitions of both polymers are due to the relaxation of their amorphous fractions, and correspond to glass transition temperatures, T_g. Therefore, an analysis of T_g of the blends allows study of miscibility in the solid state. For example, if two well defined T_gs, that are far apart from each other and that correspond to each of the original T_gs of the homopolymers, are observed, one can conclude that the blends are immiscible; if one well defined T_g is present, miscibility of both components occurred. In our case this kind of analysis is somehow more complex because the T_gs of the original homopolymers are very close to each other (120 and 105 °C), and resolution of both temperatures in the blends can be difficult. Only one well defined T_g was observed in the PPS–LCP blends; this T_g value was located between the values of the T_gs of the original homopolymers, suggesting that miscibility occurred.

Therefore, one can conclude that due to the changes with blending that the two secondary LCP transitions (β and α') experienced, and to the surging of only one T_g, miscibility of the amorphous fractions of both polymers occurred.

3.2.2. Morphology

Fig. 6 shows SEM micrographs of the fracture surfaces of the homopolymers after capillary extrusion at 1173 s^{-1}. The observed surfaces are perpendicular to the flow direction and near to the wall, as said before. Fig. 6a shows pure PPS and Fig. 6b, pure Vectra. PPS has a fragile fracture, while LCP has ductile and fibrillar surfaces. Fig. 7 shows SEM micrographs of samples A (7 min), also after capillar extrusion at 1173 s^{-1}, together with their corresponding X-ray microanalyses. The morphology of samples A (15 min) was essentially the same as samples A (7 min). This observation was similar to studies [14, 15] made in conventional blends, in which it was found that the increase of mixing time does not change the size of the dispersed phase considerably, independent of the λ value. Therefore these micrographs are not shown. In Fig. 7a, surface fracture of the 70 : 30 blend is shown; corresponding X-ray microanalyses are shown in Fig. 7b (matrix) and Fig. 7c (fibres). The X-ray microanalysis of the matrix shows the presence of S, besides the Au coating; microanalysis of the fibres also shows the presence of S. Therefore, in this blend, the formation of fibrils made of PPS and probably also LCP occurs, with diameters between 4–16 μm, embedded in a PPS-rich matrix. Fig. 7d (50 : 50 blend) shows another kind of morphology: the formation of PPS-rich fibres, 8–16 μm in diameter, embedded in a LCP-rich matrix; its corresponding X-ray microanalysis is the same as that of the 30 : 70 blends. Fig. 7e shows the fracture surface of a 30 : 70 blend; corresponding X-ray microanalyses are shown in Fig. 7f (matrix) and Fig. 7g (fibres). The microanalysis of the matrix does not show the presence of S; however, the analysis of the fibres shows a high amount of S. Therefore, as in the 50 : 50 blend, PPS-rich fibrils are formed, embedded in a LCP matrix, instead of sole LCP fibrils. The diameters of the fibres of the 30 : 70 blend are slightly smaller than the diameters of the fibres of the 50 : 50 blend. Table III shows a summary of these observations, together with the corresponding value of λ.

It can be observed that if one assumes that $\nu \to 0$, it would be expected that blend 70 : 30 would form LCP

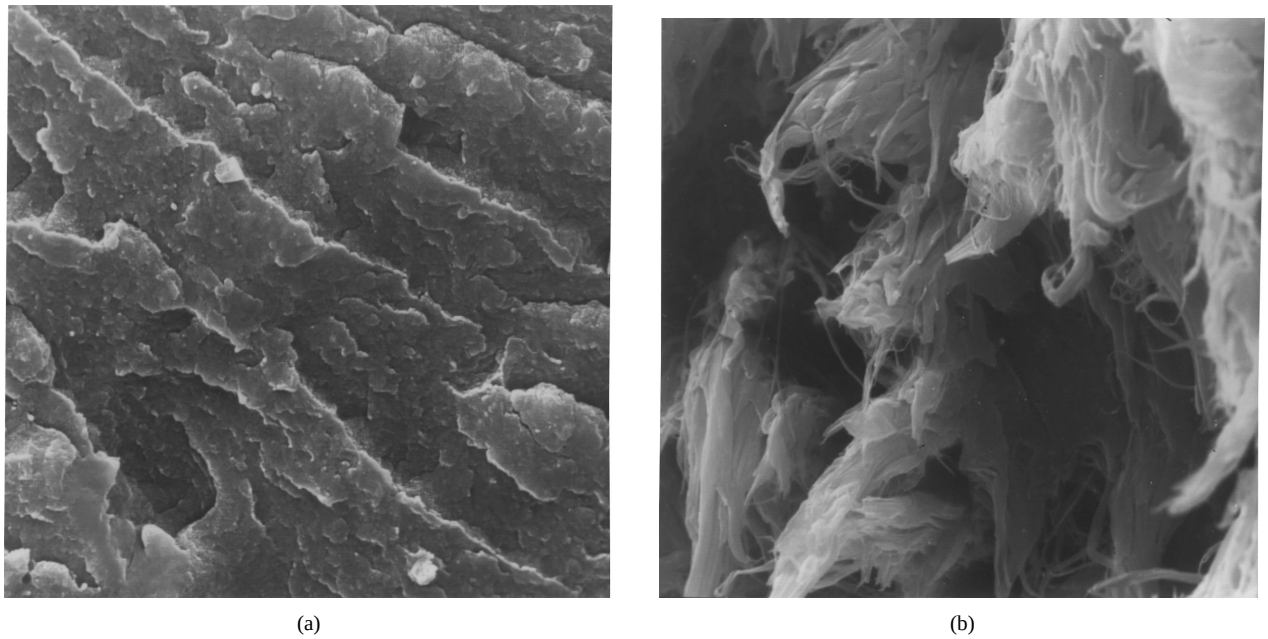

(a) (b)

Figure 6 Scanning electron micrographs of the fracture surfaces of the pure polymers after capillary extrusion at 1173 s^{-1}: (a) pure PPS, and (b) pure Vectra.

TABLE III Morphology of samples A as observed by SEM for PPS–Vectra blends

	λ	Morphology	Diameter of the dispersed phase (μm)
70 : 30	<1	Fibrils (PPS + LCP) Matrix (PPS-rich)	4–16
50 : 50		Fibrils (PPS + LCP) Matrix (LCP)	8–16
30 : 70	>1	Fibrils (PPS + LCP) Matrix (LCP)	6–10

fibrils (dispersed phase) if high shear rates were to predominate. Instead, PPS–LCP fibrils were formed due to miscibility of both polymers and to the high shear rates of capillary extrusion. In the case of the 30 : 70 blend, PPS fibrillation (dispersed phase) would occur if high extensional deformation were to predominate. Instead, fibrils of PPS and LCP were formed, also due to miscibility of both components and the high extensional rates developed at the entrance region of the capillary. Also, it was observed that, in these blends, no LCP C^* was necessary to obtain fibrillation, as already observed in other systems.

Fig. 8 shows SEM micrographs of samples B. In Fig. 8a (30 : 70 blend) a macrofibre of approximately 150 μm in diameter, made of PPS and LCP, is observed. This macrofibre is composed of microfibrils of approximately 10 μm in diameter; this structure is characteristic of LCPs. A different morphology is observed in Fig. 8b (50 : 50 blend, fibrils of 15 μm) and Fig. 8c (70 : 30 blend, fibrils of 25 μm). In these blends, the

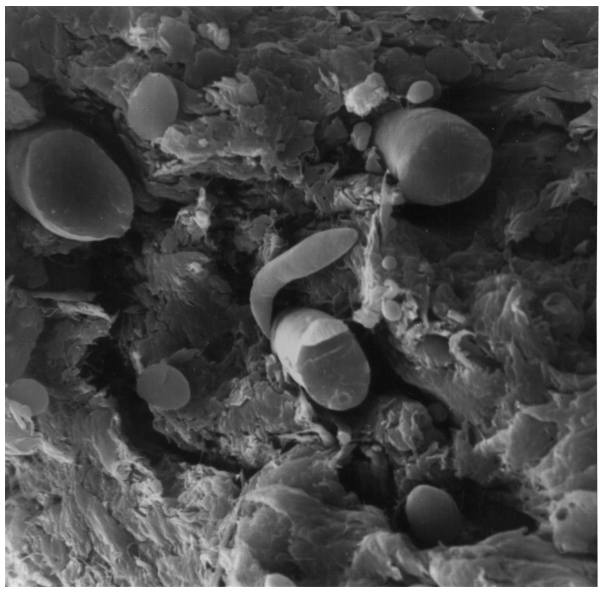

(a)

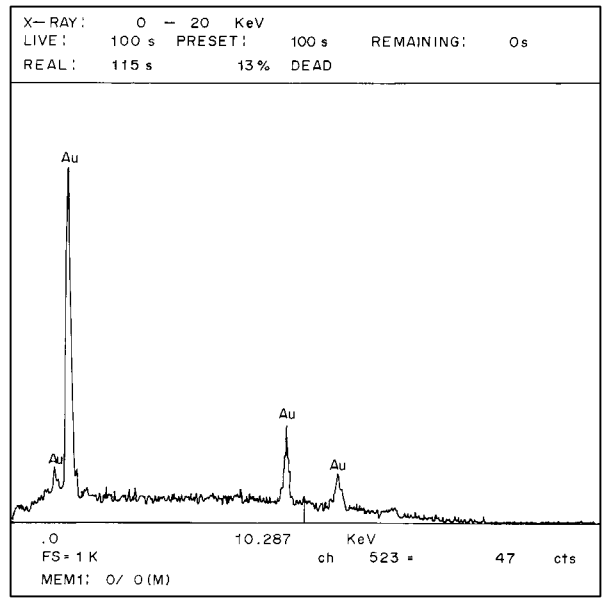

(b)

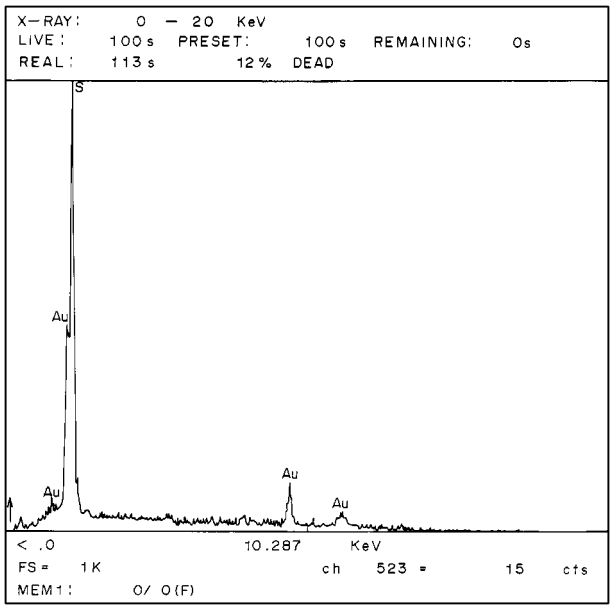

(c)

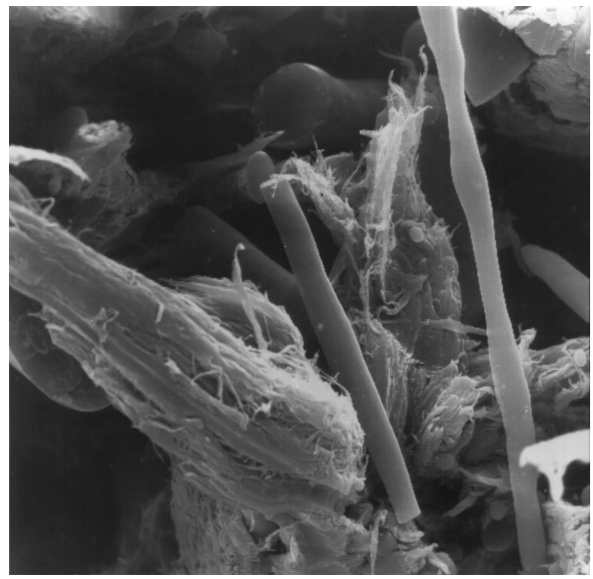

(d)

Figure 7 Scanning electron micrographs and X-ray microanalyses of samples A (7 min), after capillary extrusion at 1173 s^{-1}: (a) micrograph of the fracture surface of a 30 : 70 blend (magnification: ×1500), (b) X-ray microanalysis of the matrix of the 30 : 70 blend, (c) X-ray microanalysis of the fibres of the 30 : 70 blend, (d) micrograph of the fracture surface of a 50 : 50 blend (magnification: ×1000), (e) micrograph of the fracture surface of a 70 : 30 blend (magnification: ×1000), (f) X-ray microanalysis of the matrix of the 70 : 30 blend, and (g) X-ray microanalysis of the fibres of the 70 : 30 blend. (*Continued*).

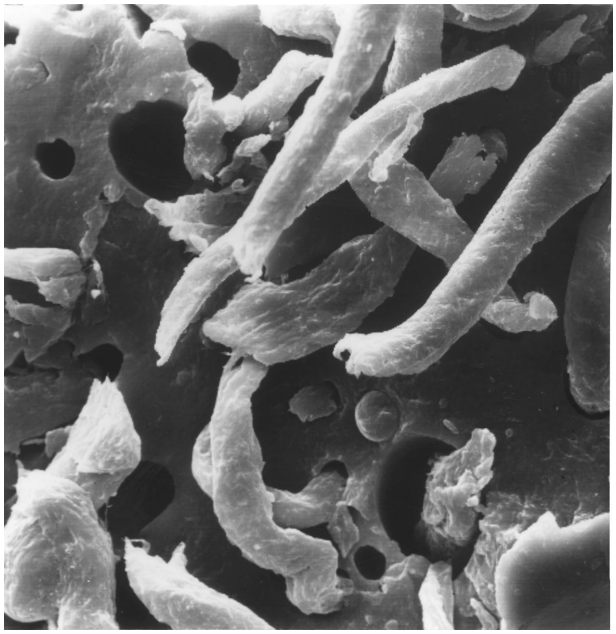

(e)

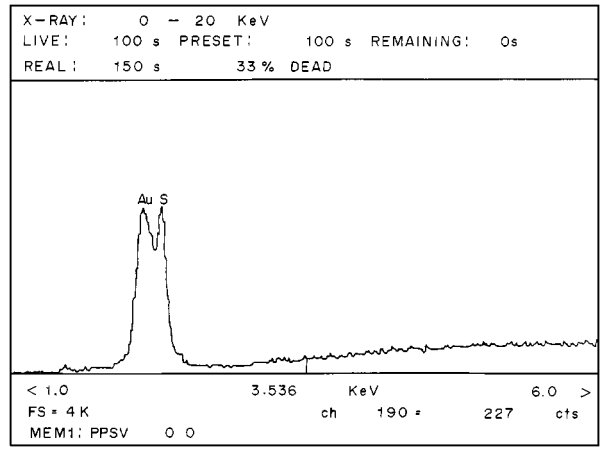

(f)

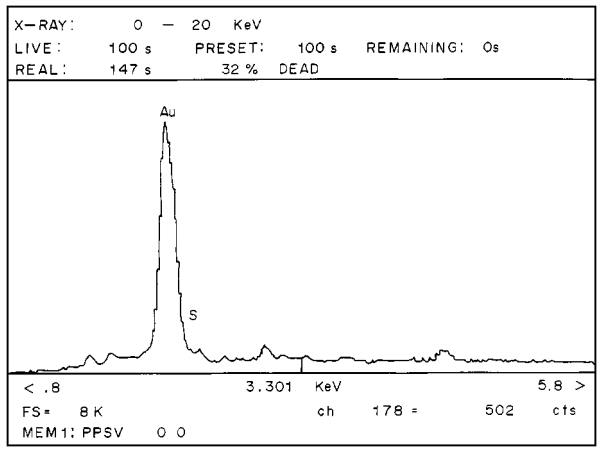

(g)

Figure 7 (*Continued*).

macrofibrils do not decompose into microfibrils, as in blend 30 : 70, due to low LCP concentration. However, in all the blends, only one homogeneous phase is observed and no distinction between "fibres" and "matrix" can be made. In injection moulding, the deformational field is more intense than in extrusion and it is composed of unsteady shear and elongational flows (due to "fountain flow"); therefore the high deformational rates characteristic of these processes are responsible for the mixing and fibrillation of both polymers, at all LCP concentrations. Table IV presents a summary of the observed morphology. These data also confirm the DMTA results: in samples B, the amorphous fractions of PPS and Vectra are miscible.

A final observation related to the morphology of these blends should be mentioned. Samples A (extruded) presented the formation of bubbles, as shown in Fig. 9; samples B (injection moulded) did not show the presence of bubbles. The surging of bubbles has been attributed [16] to reaction between the blend components. In our case, probably the high pressures employed during injection moulding did not allow surging of bubbles in samples B.

TABLE IV Morphology of samples B as observed by SEM for PPS–Vectra blends

	Morphology	Average diameter of the fibres (μm)
30 : 70	Macrofibres (PPS + LCP); microfibrils (PPS + LCP)	150 (macrofibres); 10 (microfibrils)
50 : 50	Fibrils (PPS + LCP)	15
70 : 30	Fibrils (PPS + LCP)	25

3.2.3. Mechanical properties

Table V shows the tensile and impact properties of the blends (samples B). The standard deviation of each average is given in parentheses.

It can be observed that the addition of LCP to PPS reinforces this last polymer; it increases PPS ultimate tensile strength, elongation to break and impact resistance. This improvement in mechanical properties can be attributed to the formation of fibrillar structures made

(a)

(b)

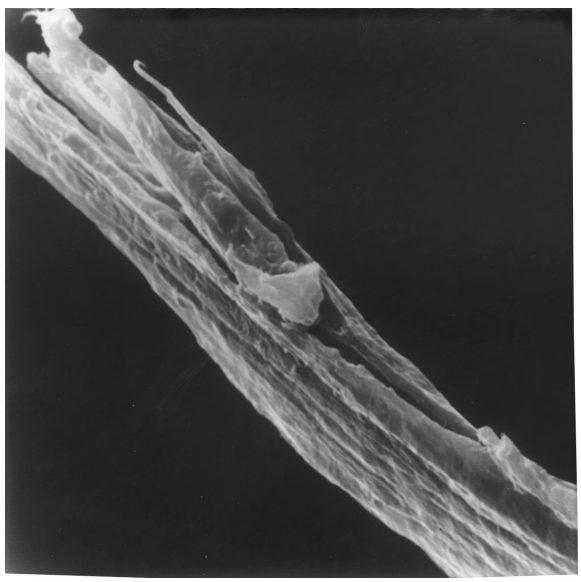

(c)

Figure 8 Scanning electron micrographs of the fracture surfaces of samples B: (a) 30 : 70 PPS–LCP blend (magnification: ×200), (b) 50 : 50 PPS–LCP blend (magnification: ×2000), and (c) 70 : 30 PPS–LCP blend (magnification: ×1000).

TABLE V Tensile and impact properties of the PPS–Vectra blends

	Ultimate tensile strength, σ_b (MPa)	Elongation at break, ε_b (%)	Impact resistance (lb ft in^{-1})
0 : 100	174.90 (10.59)	18.41 (0.72)	3.26 (0.44)
30 : 70	105.14 (13.6)	9.12 (0.13)	2.56 (0.94)
50 : 50	103.28 (6.73)	5.66 (0.9)	1.28 (0.61)
70 : 30	99.75 (8.74)	5.59 (0.32)	0.43 (0.28)
100 : 0	64.37 (5.48)	4.66 (0.23)	0.20 (0.04)

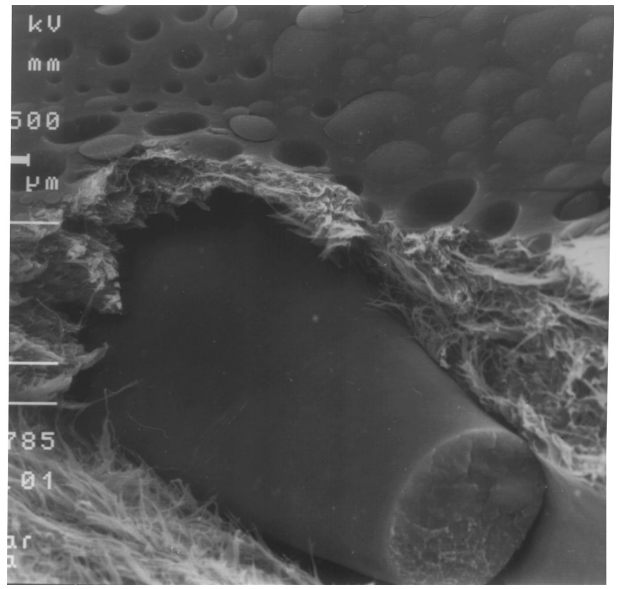

Figure 9 Scanning electron micrograph of sample A (30 : 70 blend; magnification: ×1000).

of both components. In this sense, PPS and Vectra A950 form a "molecular composite".

4. Conclusions

From this preliminary study, it is possible to conclude:

1. PPS–Vectra blends are miscible in the melt and solid states. The intensity of the miscibility will depend on the intensity of the applied deformational flow field. In capillary extrusion, the formation of fibrils made of both components is observed; however, the matrixes seem to be made of a sole polymer (PPS or LCP). In injection moulding, fibrils and matrix are made of both components.

2. The formation of pure LCP fibrils was not observed, neither in the extruded blends nor in the injection moulded samples. Therefore, no LCP C^* was necessary for fibrillation, as already observed in other LCP blends.

3. The addition of Vectra to PPS improves its mechanical properties, due to the formation of fibrillar morphologies, made of both components. At a molecular level, these blends can be considered "molecular composites".

Acknowledgements

This research was supported by Volskwagen Foundation (I-69693) and FAPESP (94/2317-9). The authors

wish to express their gratitude to Hoechst S. A. of Brasil for donation of the polymers.

References

1. D. G. BAIRD, T. SUN, D. S. DONE and R. RAMANATHAN, *ACS Polym. Chem. Polym. Prepr.* **30** (1989) 546.
2. A. I. ISAYEV and M. MODIC, *Polym. Comp.* **3** (1987) 159.
3. W. S. CARVALHO and R. E. S. BRETAS, *Eur. Polym. J.* **26** (1990) 817.
4. R. E. S. BRETAS, D. COLLIAS and D. G. BAIRD, *Polym. Eng. Sci.* **34** (1994) 1492.
5. R. E. S. BRETAS and D. G. BAIRD, *Polymer* **33** (1992) 24, 5233.
6. M. T. HEINO and J. V. SEPPALA, *J. Appl. Polym. Sci.* **44** (1992) 1051.
7. A. M. SUKAHADIA, D. DONE and D. G. BAIRD, *Polym. Eng. Sci.* **30** (1990) 519.
8. B. CARVALHO, G. GABELLINI and R. E. S. BRETAS, *Polímeros: Ciencia e Tecnologia* **V** (1995) 31.
9. G. GABELLINI, M. MORAES and R. E. S. BRETAS, *J. Appl. Polym. Sci.* **60** (1996) 21.
10. G. GABELLINI and R. E. S. BRETAS, *ibid.* **61** (1996) 1083.
11. B. CARVALHO and R. E. S. BRETAS, *ibid.* **55** (1995) 233.
12. M. A. GOMEZ, C. MARCO, J. M. G. FATOU, N. SUAREZ, E. LAREDO and A. BELLO, *J. Appl. Polym. Sci., Polym. Phys.* **33** (1995) 1259.
13. B. CULBERLSON (Ed.) "Contemporary Topics in Polymer Science, Multiphase Macromolecular Systems," Vol. 6 (Plenum Press, New York, 1989).
14. A. P. PLOCHOKI, S. S. DAGLI and R. D. ANDREWS, *Polym. Eng. Sci.* **30** (1990) 741.
15. B. D. FAVIS, *J. Appl. Polym. Sci.* **39** (1990) 25.
16. R. RAMANATHAN, K. BLIZARD and D. G. BAIRD, *SPE ANTEC* **34** (1988) 1123.

Received 12 September 1997
and accepted 1 September 1998